Current and Voltage Reconstruction from Non-Contact Field Measurements

David Lawrence, John Donnal, and Steven Leeb

***Abstract*—Non-contact electromagnetic field sensors can monitor voltage and current in multiple-conductor cables from a distance. Knowledge of the cable and sensor geometry is generally required to determine the transformation that recovers voltages and currents from the sensed electromagnetic fields. This paper presents a new calibration technique that enables the use of non-contact sensors without prior knowledge of conductor geometry. Calibration of the sensors is accomplished with a reference load or through observation of *in situ* loads.**

***Index Terms*—Sensor systems, magnetic sensors**

I. Introduction

An electric current flowing through a conductor produces a magnetic field whose magnitude at any point in space is proportional to the current. Similarly, a voltage applied to a conductor produces an electric field whose magnitude is proportional to the voltage. The voltage and current in a conductor may thus be determined by electric and magnetic field sensors placed nearby [1], [2]. The obvious appeal of this technique is that it works at a distance, i.e. it is not necessary to remove the insulation from a wire in order to measure its voltage and current [3]. Non-contact sensors have a lower cost of installation because they do not require power to be shut down by an electrician.

Figure 1 illustrates a hardware implementation of a non-contact sensing system developed for this paper. A utility service entry cable is shown in the figure. Each one of the four sensors shown in the figure (secured to the cable) can make a measurement of electric and magnetic field at that point on the cable. Three such sensor "heads" are labeled in Fig. 1 as measuring field quantities S_1, S_2, and S_3. Up to four sensor heads can be connected to a digital coordination board, which samples the current and voltage sensors on each head. Data from the sensor heads can be read at sample rates up to 3 kHz and transmitted over a USB serial connection to a computer. The sensor heads are carefully constructed with permalloy and ground shielding to ensure that electric and magnetic field measurements are "focused" on the cable and that interference from external fields is minimized or eliminated, as described in [6].

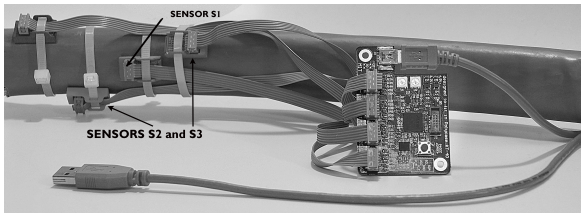

Fig. 1. Non-contact meter using capacitive voltage sensors and magnetic current sensors installed on a service entrance cable for nonintrusive monitoring.

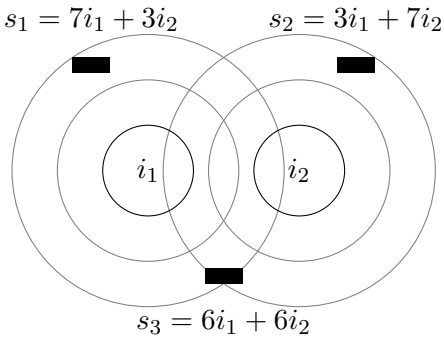

Fig. 2. Schematic of non-contact sensor deployment with two conductors and three sensors. In the text, quantities s_1, s_2, and s_3 represent magnetic field strengths. The quantities i_1 and i_2 are currents.

When a cable like the one shown in Fig. 1 contains multiple conductors, the electric and magnetic fields from each conductor superpose. Thus, a magnetic field sensor records a linear combination of the currents through each conductor (as depicted in the cross-sectional schematic view shown in Fig. 2) and an electric field sensor records a linear combination of the voltages on each conductor. The black rectangles in Fig. 2 provide a schematic representation of the sensor heads shown in Fig. 1. These sensor heads read magnetic fields that are produced by the currents i_1 and i_2 in the center circles of Fig. 2. The concentric circles around each current schematically represent the magnetic field lines created by the wire currents. Each magnetic field reading from an individual sensor will be a linear combination of the scaled currents i_1 and i_2, as indicated by the representative equations for S_1, S_2, and S_3 in Fig. 2.

With enough sensors in different locations, the linear transformation from cable currents and voltages to sensor readings is invertible and the original currents and voltages may be recovered [4], [5]. The process of determining the transformation from sensor readings to voltages and currents is called "calibration". Reference [1] introduced an algorithm for calibrating non-contact sensors to recover estimates of wire currents in a cable. This process involves introducing a calibration load on each phase or conductor in the wire bundle in seriatim.

As described in [1], a suitable calibration load might be a resistive load switched on and off at a controlled duty cycle for a minute or two on each phase of the power service. In a residence, for example, this would involve plugging in a resistive load switched on and off by a solid-state relay for a window of time, and then performing the experiment again on the "other" phase in the house (assuming a home with a split-phase service). The switching permits the calibration load to be uniquely detected on each phase during calibration, even while other loads are operating. With a known number of conducting phases, and an equal number of installed sensor heads, and a careful but relatively easy set of quick experiments plugging in a calibration load once on each phase, the matrix relating sensor measurements to cable currents can be uniquely determined. After calibration, the sensor measurements can be used as a henceforth "non-contact" estimator for the cable currents.

This paper expands the algorithm of [1] to provide the following new capabilities:

1) The number of sensors may be made larger than the number of conductors, and accuracy is improved by each additional sensor.
2) The mathematics remain computationally tractable even with a large number of sensors.
3) The calibration technique is extended to the case of three-phase delta-connected power distribution.
4) Calibration may be completed up to a constant scaling factor multiplying each current without the use of a reference load. The scaling factor is then determined by comparison with the utility power meter over a longer period of time.
5) Because overconstraint is handled by the algorithms described in this paper, if a reference load or other known load is used, it may be attached to each conductor multiple times, and it is not necessary to know which conductor is connected each time.

The paper begins by developing these extensions of the calibration algorithm for DC systems that have an external path for return currents. The algorithm is then further generalized to handle AC systems, systems without an external path for return currents, and three-phase delta-connected AC systems. Lastly, the algorithm is modified to use observation of *in situ* loads in place of a reference load.

II. Calibration algorithm

This section considers the case of DC systems that have an unmonitored conductor to carry return currents. For example, most automobiles use 12 V DC distribution wires and return currents through the metal chassis. This section also assumes the use of a known reference load. The reference load is switched at a particular frequency and the demodulation scheme of [1] is used to distinguish it from any other loads which are present.

Suppose that there are k magnetic field sensors monitoring a cable with n conductors. The currents through the cable at time t are

$$\boldsymbol{i}(t) = \begin{bmatrix} i_1(t) \\ \vdots \\ i_n(t) \end{bmatrix}$$

and the sensed magnetic fields are

$$\boldsymbol{s}(t) = \begin{bmatrix} s_1(t) \\ \vdots \\ s_k(t) \end{bmatrix}.$$

Each sensor detects a mixture of the magnetic fields due to each current, so the sensor geometry and the laws of physics determine a k-by-n matrix $\boldsymbol{M}$ satisfying

$$\boldsymbol{s}(t) = \boldsymbol{M}\boldsymbol{i}(t). \tag{1}$$

The goal of calibration is to find an n-by-k matrix $\boldsymbol{K}$ satisfying

$$\boldsymbol{i}(t) = \boldsymbol{K}\boldsymbol{s}(t) \tag{2}$$

using no information other than measurements of $\boldsymbol{s}$. Throughout this paper, lowercase boldface letters will refer to column vectors and uppercase boldface letters will refer to matrices.

If $k < n$, such a $\boldsymbol{K}$ does not exist. This situation is resolved by adding additional sensors. If $k \geq n$, matrix $\boldsymbol{K}$ is chosen to be the pseudoinverse of $\boldsymbol{M}$. This $\boldsymbol{K}$ has the smallest condition number of any left inverse of $\boldsymbol{M}$, so it minimizes the sensitivity of the unmixed currents to electromagnetic noise and physical perturbations. In general, the pseudoinverse of a matrix $\boldsymbol{M}$ will be denoted by $\boldsymbol{M}^+$.

The matrix $\boldsymbol{K} = \boldsymbol{M}^+$ is decomposed into a product $\boldsymbol{M}^+ = \boldsymbol{U}\boldsymbol{D}$ such that $\boldsymbol{U}$ is an invertible n-by-n matrix and $\boldsymbol{D}$ is an n-by-k matrix whose rows are orthonormal.

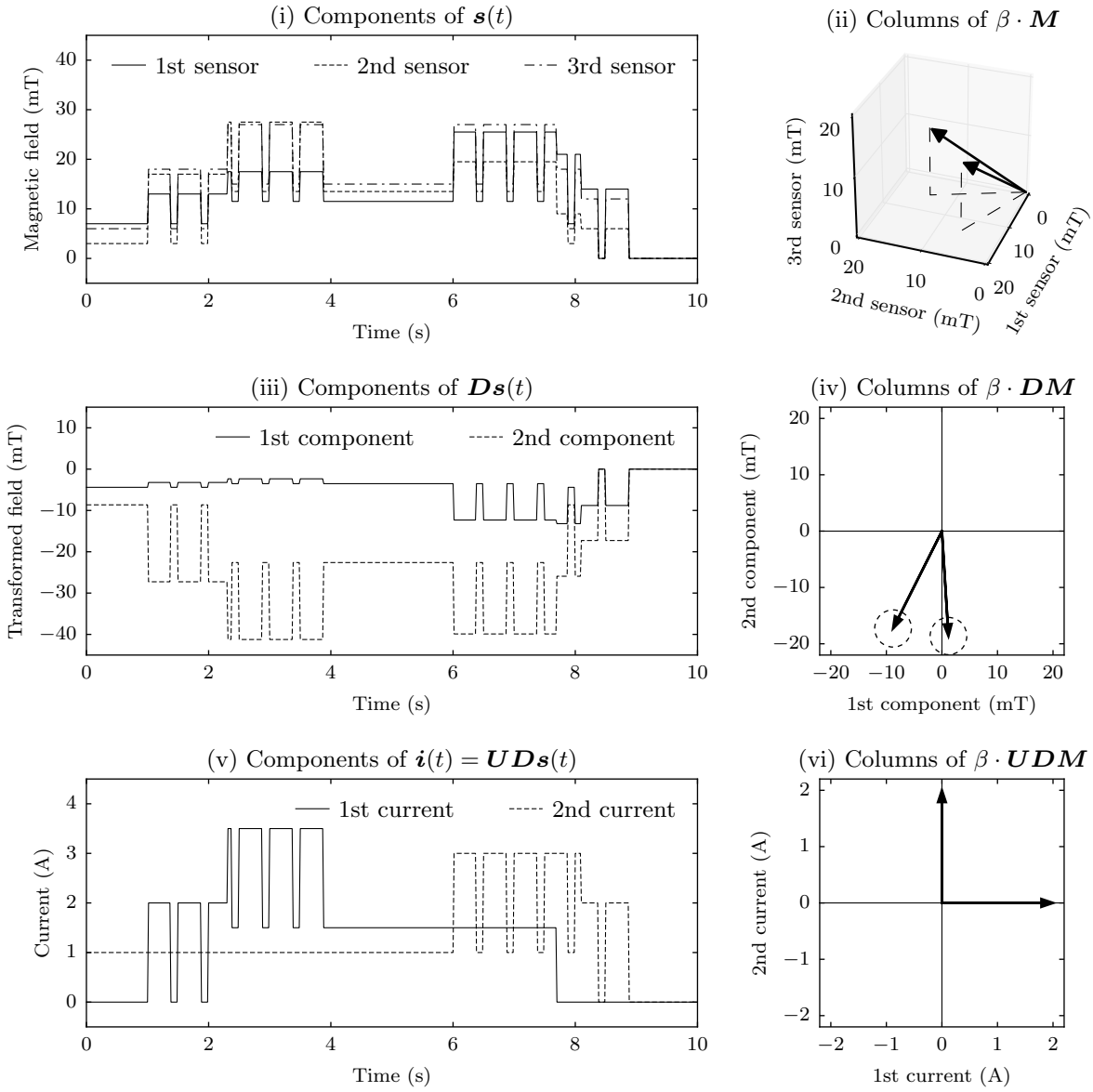

Fig. 3. Graphical depiction of the unmixing procedure proceeding simultaneously in the time domain and in vector space. As depicted in Fig. 2, there are three sensors and two conductors. The reference load draws a current of $\beta = 2\,\text{A}$ modulated at 2 Hz on the first conductor for $1 < t < 4$ and on the second conductor for $6 < t < 9$. There is an additional current of $\beta = 1.5\,\text{A}$ on the first conductor for $2.3 < t < 7.7$ and an additional current of 1 A on the second conductor for $t < 8.1$.

Fig. 3 illustrates the behavior of this decomposition for the system of Fig. 2. To begin with, Fig. 3(i) depicts ten seconds of simulated sensor readings. Multiplication by $\boldsymbol{D}$ reduces the sensor readings from three dimensions to two, as shown in Fig. 3(iii). Finally, multiplication by $\boldsymbol{U}$ recovers the original conductor currents, as shown in Fig. 3(v).

Suppose that the reference load such as a power resistor that draws a current of β which is modulated at a particular frequency and duty cycle by a solid-state relay. This combination, a resistor and a solid-state relay cycled by a microcontroller, provides a typical calibration load for our field work. Fig. 3(v) depicts a reference load with $\beta = 2\,\text{A}$ that is modulated at 2 Hz with a 75% duty cycle in the presence of background loads. When the reference load is attached to the xth conductor, it draws a modulated current of $\beta\hat{\boldsymbol{i}}_x$ (where $\hat{\boldsymbol{i}}_x$ denotes the xth basis current, i.e. the length-n vector with a 1 in the xth position and zeros everywhere else). The resulting magnetic field is $\boldsymbol{M} \cdot \beta\hat{\boldsymbol{i}}_x$—in other words, it is equal to β times the xth column of $\boldsymbol{M}$. Fig. 3(ii) depicts these magnetic field vectors for a 2 A reference load used with the system of Fig. 2.

In general, the demodulation algorithm of [1] is used

to detect the presence of the reference load and determine the sensed magnetic fields which are due to each current that it draws. Suppose that p runs of the reference load are detected (where $p \geq n$) and that the demodulated sensor readings in the xth run are equal to $\boldsymbol{\sigma}_x$. If the reference load switches on at time t_x, then

$$\boldsymbol{\sigma}_x = \boldsymbol{s}(t_x + \epsilon) - \boldsymbol{s}(t_x - \epsilon)$$

for a sufficiently small value of ϵ. The demodulation algorithm is simply a more robust method of determining this quantity in the presence of other loads.

After the reference load has been attached to every conductor, the k-by-p matrix

$$\boldsymbol{\Sigma} = \begin{bmatrix} \boldsymbol{\sigma}_1 & \cdots & \boldsymbol{\sigma}_p \end{bmatrix} \tag{3}$$

is assembled and the eigendecomposition of the k-by-k matrix $\boldsymbol{\Sigma}\boldsymbol{\Sigma}'$ is computed. Because $\boldsymbol{\Sigma}\boldsymbol{\Sigma}'$ is Hermitian positive semidefinite, its eigenvalues are non-negative real numbers and its eigenvectors are orthonormal. Suppose that the eigendecomposition is given by

$$\boldsymbol{\Sigma}\boldsymbol{\Sigma}' = \begin{bmatrix} \boldsymbol{\rho}_1 & \cdots & \boldsymbol{\rho}_k \end{bmatrix} \begin{bmatrix} \lambda_1 & & 0 \\ & \ddots & \\ 0 & & \lambda_k \end{bmatrix} \begin{bmatrix} \boldsymbol{\rho}_1' \\ \vdots \\ \boldsymbol{\rho}_k' \end{bmatrix} \tag{4}$$

where the $\boldsymbol{\rho}_x$ are orthonormal k-element column vectors and $\lambda_x \geq \lambda_{x+1}$.

Although the columns of $\boldsymbol{\Sigma}$ are k-dimensional vectors, they all correspond to valid sensor readings and so they all lie in an n-dimensional subspace defined by the image of $\boldsymbol{M}$. Therefore the rank of $\boldsymbol{\Sigma}$ is equal to n, and $\lambda_x = 0$ for $x > n$. In practice, any noise added to the sensor readings may increase these eigenvalues to be slightly greater then zero. Reference [6] proves that the gap between the smallest nonzero eigenvalue and the largest zero eigenvalue is bounded by the signal-to-noise ratio of the sensors, so counting the nonzero eigenvalues of $\boldsymbol{\Sigma}\boldsymbol{\Sigma}'$ is a robust method to determine n.

The eigendecomposition of $\boldsymbol{\Sigma}\boldsymbol{\Sigma}'$ also provides the matrix

$$\boldsymbol{D} = \begin{bmatrix} \boldsymbol{\rho}_1 & \cdots & \boldsymbol{\rho}_n \end{bmatrix}'. \tag{5}$$

Reference [6] proves that there exists an invertible $\boldsymbol{U}$ such that $\boldsymbol{M}^+ = \boldsymbol{U}\boldsymbol{D}$, and furthermore, that $\boldsymbol{M}^+$ is the *only* left inverse of $\boldsymbol{M}$ which may be written as a product of a matrix $\boldsymbol{U}$ with this $\boldsymbol{D}$. Fig. 3(iv) illustrates that $\boldsymbol{D}$ projects the columns of $\boldsymbol{M}$ to an n-dimensional subspace while preserving their lengths and the angles between them. All that remains is to find the matrix $\boldsymbol{U}$.

A spectral clustering algorithm [7] is used to group the vectors $\boldsymbol{\sigma}_x$ by conductor. The distance function d used by the clustering algorithm is the angle between the lines spanned by two reference load signatures, i.e.

$$d(\boldsymbol{\sigma}_x, \boldsymbol{\sigma}_y) = \arccos\left(\frac{\|\boldsymbol{\sigma}_x'\boldsymbol{\sigma}_y\|}{\|\boldsymbol{\sigma}_x\|\|\boldsymbol{\sigma}_y\|}\right). \tag{6}$$

Because $\boldsymbol{D}$ preserves the angles between reference signatures,

$$d(\boldsymbol{\sigma}_x, \boldsymbol{\sigma}_y) = d(\boldsymbol{D}\boldsymbol{\sigma}_x, \boldsymbol{D}\boldsymbol{\sigma}_y)$$

and the clustering can be performed in n-dimensional space. The elements of this space are expected to be clustered near columns of $\beta \cdot \boldsymbol{D}\boldsymbol{M}$, as indicated by the dashed regions in Fig. 3(iv).

Suppose that the clustering algorithm partitions $\boldsymbol{D}\boldsymbol{\sigma}_1, \ldots, \boldsymbol{D}\boldsymbol{\sigma}_p$ into n clusters and selects a representative element $\boldsymbol{\delta}_x$ for the xth cluster. Because the xth cluster corresponds to the xth conductor, the reference load currents are given by

$$\beta\hat{\boldsymbol{i}}_x = \boldsymbol{U}\boldsymbol{\delta}_x.$$

This equation is solved for $\boldsymbol{U}$ to obtain

$$\boldsymbol{U} = \beta \begin{bmatrix} \boldsymbol{\delta}_1 & \cdots & \boldsymbol{\delta}_n \end{bmatrix}^{-1}. \tag{7}$$

Then

$$\boldsymbol{K} = \boldsymbol{U}\boldsymbol{D} \tag{8}$$

and calibration is finished. Fig. 3(vi) shows that multiplying $\beta\boldsymbol{M}$ by $\boldsymbol{U}\boldsymbol{D}$ on the left recovers the original reference currents $\beta\hat{\boldsymbol{i}}_x$.

Algorithm 1 Calibration for direct currents with external path for return current.

Require: each reference load signature present in $\boldsymbol{s}$ is equal to β times a column of some matrix $\boldsymbol{M}$, and all columns of $\boldsymbol{M}$ are represented by reference load signatures.

Ensure: $\boldsymbol{K}$ is the pseudoinverse of $\boldsymbol{M}$, up to a permutation of its rows.

function CALIBRATE($\boldsymbol{s}$, β)
  $\boldsymbol{\sigma}_* \leftarrow$ FINDREFERENCELOADS($\boldsymbol{s}$)
  $\boldsymbol{\Sigma} \leftarrow \begin{bmatrix} \boldsymbol{\sigma}_1 & \cdots & \boldsymbol{\sigma}_p \end{bmatrix}$
  $\lambda_*, \boldsymbol{\rho}_* \leftarrow$ EIGENDECOMPOSITION($\boldsymbol{\Sigma}\boldsymbol{\Sigma}'$)
  $n \leftarrow$ COUNTNONZERO($\lambda_1, \ldots, \lambda_k$)
  $\boldsymbol{D} \leftarrow \begin{bmatrix} \boldsymbol{\rho}_1 & \cdots & \boldsymbol{\rho}_n \end{bmatrix}'$
  $\boldsymbol{\delta}_* \leftarrow$ SPECTRALCLUSTER($\boldsymbol{D}\boldsymbol{\sigma}_1, \ldots, \boldsymbol{D}\boldsymbol{\sigma}_p$)
  $\boldsymbol{U} \leftarrow \beta \begin{bmatrix} \boldsymbol{\delta}_1 & \cdots & \boldsymbol{\delta}_n \end{bmatrix}^{-1}$
  $\boldsymbol{K} \leftarrow \boldsymbol{U}\boldsymbol{D}$
  return $\boldsymbol{K}$
end function

Algorithm 1 summarizes the method for determining $\boldsymbol{M}^+$ from $\boldsymbol{s}$ that was derived in this section. In summary, it is used in the following manner:

1) Attach a reference load which draws a constant current of β to each conductor of the instrumented cable in turn.
2) Call the function CALIBRATE$(\boldsymbol{s}, \beta)$, where $\boldsymbol{s}$ is a range of sensor data that includes all of the reference load runs. The result is the matrix $\boldsymbol{M}^+$.
3) To perform regular monitoring of currents, multiply the sensed magnetic field $\boldsymbol{s}(t)$ by $\boldsymbol{M}^+$ on the left to obtain the current $\boldsymbol{i}(t)$.

III. Alternating currents

The calibration algorithm is next extended to the case of AC systems. The same algorithm that was developed for DC systems is applied to the Fourier transform of the AC sensor data. An important difference is that the Fourier transform is complex-valued and includes both magnitude and phase information. In this section, it is still assumed that an unmonitored conductor carries the return currents and that a modulated reference load is used for calibration. The AC reference load is a resistive device, i.e. when it is switched on it draws an alternating current that is in phase with the applied voltage.

The Fourier transform $\mathcal{F}$ is defined by

$$\big(\mathcal{F}_y(f)\big)(t) = \sqrt{2}\int_0^1 f(t - T\tau)e^{2\pi i j\tau}\, d\tau \qquad (9)$$

where T denotes the period of the alternating current. In other words, $\mathcal{F}_y(f)$ is the yth Fourier coefficient of f over a sliding window with a length of one period. The normalization factor is chosen so that the magnitude of $\mathcal{F}_y(f)$ is equal to the RMS amplitude of the corresponding sinusoid.

The power transmission over one period is defined as

$$p_x(t) = \mathcal{F}_1(v_x)(t) \cdot \overline{\mathcal{F}_1(i_x)(t)},$$

where the real part of p_x is the real power transmitted on the xth conductor and the imaginary part of p_x is the reactive power on the xth conductor. Suppose that the phase of the voltage $v_x(t)$ on the xth conductor is θ_x, so that

$$v_x(t) = A_x \cos(2\pi t/T + \theta_x).$$

The amplitude A_x is known in advance, so the calibration procedure is only responsible for determining the rotated current

$$c_x(t) = \frac{p_x(t)}{|\mathcal{F}_1(v_x)(t)|} = e^{2\pi j t/T + j\theta_x} \cdot \overline{\mathcal{F}_1(i_x)(t)}.$$

This equation can be written in vector form as

$$\boldsymbol{c}(t) = e^{2\pi j t/T} \cdot \boldsymbol{\Theta} \cdot \overline{\mathcal{F}_1(\boldsymbol{i})(t)} \qquad (10)$$

where

$$\boldsymbol{\Theta} = \begin{bmatrix} e^{j\theta_1} & & 0 \\ & \ddots & \\ 0 & & e^{j\theta_n} \end{bmatrix}.$$

It happens that $\boldsymbol{c}(t)$ is directly related to the Fourier transforms of the sensed magnetic fields. These transforms are given by

$$\boldsymbol{b}(t) = e^{2\pi j t/T} \cdot \overline{\mathcal{F}_1(\boldsymbol{s})(t)} \qquad (11)$$

where $e^{2\pi j t/T}$ is a phase shift to compensate for the alignment of the transform window. Since $\mathcal{F}_1$ is a linear operator, equation (1) implies that

$$\overline{\mathcal{F}_1(\boldsymbol{s})(t)} = \boldsymbol{M} \cdot \overline{\mathcal{F}_1(\boldsymbol{i})(t)}. \qquad (12)$$

Combine (10), (11), and (12) to obtain

$$\boldsymbol{b}(t) = \boldsymbol{M}\boldsymbol{\Theta}'\boldsymbol{c}(t) \qquad (13)$$

and the inverse relation

$$\boldsymbol{c}(t) = \boldsymbol{\Theta}\boldsymbol{M}^+\boldsymbol{b}(t). \qquad (14)$$

Equations (13) and (14) are analogous to (1) and (2) from the DC case.

In order to compute $\boldsymbol{b}$ from $\boldsymbol{s}$, it is necessary to deduce $e^{2\pi j t/T}$ from measurements of the conductor voltages. (This prevents the inevitable problem of clock skew between the supposed time t and the actual phases of the voltages.) Suppose that a capacitively-coupled non-contact voltage sensor [1] is used to measure an arbitrary mixture $v_m(t)$ of the conductor voltages. Since the the time t may be shifted by any constant factor, suppose without loss of generality that $v_m(t)$ is a "zero phase" signal, i.e.

$$\frac{\mathcal{F}_1(v_m)(t)}{|\mathcal{F}_1(v_m)(t)|} = e^{2\pi j t/T}. \qquad (15)$$

Equations (11) and (15) are combined to obtain

$$\boldsymbol{b}(t) = \frac{\mathcal{F}_1(v_m)(t)}{|\mathcal{F}_1(v_m)(t)|} \cdot \overline{\mathcal{F}_1(\boldsymbol{s})(t)} \qquad (16)$$

which allows $\boldsymbol{b}(t)$ to be determined without the need for a synchronized clock.

With this framework in place, an AC system is easily calibrated using algorithm 1:

1) Attach a reference load which draws a constant-amplitude sinusoidal current of β (in phase with the voltage) to each conductor of the instrumented cable in turn.
2) Use (16) to compute $\boldsymbol{b}$ over an interval of time which includes all runs of the reference load.
3) Call the function CALIBRATE$(\boldsymbol{b}, \beta)$. The result is the matrix $\boldsymbol{\Theta}\boldsymbol{M}^+$.

4) To perform regular monitoring of currents, compute $\boldsymbol{b}(t)$ from $\boldsymbol{s}(t)$ using (16). Then multiply by $\boldsymbol{\Theta}\boldsymbol{M}^+$ on the left to obtain the desired output $\boldsymbol{c}(t)$.

In other words, the DC calibration procedure seamlessly handles AC phase shifts when it is applied to complex-valued signals.

IV. Return currents

This section extends the DC and AC calibration algorithms to the common case where the currents through a multiple-conductor cable are required to sum to zero. For example, in residential AC distribution systems, any current drawn through one of the line conductors is returned through the neutral conductor. We begin by considering the DC case. Suppose that $i_1(t), \ldots, i_{n-1}(t)$ are the supply currents and $i_n(t)$ is the return current. The reduced-length current vector is defined by

$$\boldsymbol{i}_r(t) = \begin{bmatrix} i_1(t) \\ \vdots \\ i_{n-1}(t) \end{bmatrix}.$$

and includes the supply currents but not the return current. Using the constraint that $i_1(t) + \cdots + i_n(t) = 0$,

$$\boldsymbol{i}(t) = \boldsymbol{H}\boldsymbol{i}_r(t) \tag{17}$$

where

$$\boldsymbol{H} = \begin{bmatrix} 1 & & 0 \\ & \ddots & \\ 0 & & 1 \\ -1 & \cdots & -1 \end{bmatrix}.$$

Combine (1) and (17) to obtain

$$\boldsymbol{s}(t) = \boldsymbol{M}\boldsymbol{H}\boldsymbol{i}_r(t) \tag{18}$$

and the inverse relation

$$\boldsymbol{i}_r(t) = (\boldsymbol{M}\boldsymbol{H})^+\boldsymbol{s}(t). \tag{19}$$

This is exactly the setup needed to apply algorithm 1:

1) Attach a reference load which draws a constant current of β to each supply conductor in turn. The return conductor always returns a current of $-\beta$.
2) Call the function CALIBRATE$(\boldsymbol{s}, \beta)$, where $\boldsymbol{s}$ is a range of sensor data that includes all of the reference load runs. The result is the matrix $(\boldsymbol{M}\boldsymbol{H})^+$.
3) To perform regular monitoring of currents, multiply the sensed magnetic fields $\boldsymbol{s}(t)$ by $(\boldsymbol{M}\boldsymbol{H})^+$ on the left to obtain $\boldsymbol{i}_r(t)$.

The only difference when a return conductor is present is that the result of calibration is $\boldsymbol{i}_r$ instead of $\boldsymbol{i}$.

The method is similar for the AC case. Analogous to (10), define the reduced-length rotated currents

$$\boldsymbol{c}_r(t) = e^{2\pi j t/T} \cdot \boldsymbol{\Theta} \cdot \overline{\mathcal{F}_1(\boldsymbol{i}_r)(t)}. \tag{20}$$

Combine (11), (18), and (20) to obtain

$$\boldsymbol{b}(t) = \boldsymbol{M}\boldsymbol{H}\boldsymbol{\Theta}'\boldsymbol{c}_r(t) \tag{21}$$

and the inverse relation

$$\boldsymbol{c}_r(t) = \boldsymbol{\Theta}(\boldsymbol{M}\boldsymbol{H})^+\boldsymbol{b}(t). \tag{22}$$

Once again, we apply algorithm 1:

1) Attach a reference load which draws a constant-amplitude current of β (in phase with the voltage) to each line conductor in turn. The neutral conductor always returns a current of amplitude β that is 180 degrees out of phase with the line voltage.
2) Use (16) to compute $\boldsymbol{b}$ over an interval of time which includes all runs of the reference load.
3) Call the function CALIBRATE$(\boldsymbol{b}, \beta)$. The result is the matrix $\boldsymbol{\Theta}(\boldsymbol{M}\boldsymbol{H})^+$.
4) To perform regular monitoring of currents, compute $\boldsymbol{b}(t)$ from $\boldsymbol{s}(t)$ using (16). Then multiply by $\boldsymbol{\Theta}(\boldsymbol{M}\boldsymbol{H})^+$ on the left to obtain $\boldsymbol{c}_r(t)$.

The only difference when a return conductor is present is that the result of calibration is $\boldsymbol{c}_r$ instead of $\boldsymbol{c}$.

V. AC delta-connected systems

In the special case of AC delta-connected power distribution systems, the conductor currents are required to sum to zero, but there is no designated return conductor. None of the conductors are at zero potential. A reference load must be attached between two line conductors, and draws a current that is in phase with the difference between the two voltages but out of phase with either of the individual voltages.

For example, consider a three-phase system. The voltages on all three conductors have the same amplitude, but the voltages on any pair of conductors are separated in phase by 120 degrees. Suppose that ϕ_x is the phase of the voltage signal $v_x(t)$, θ_1 is the phase of the difference $v_1(t) - v_3(t)$, and θ_2 is the phase of the difference $v_2(t) - v_3(t)$.

A reference load is first attached between conductors 1 and 3, and then between conductors 2 and 3. The previous algorithm for AC systems produces $\boldsymbol{c}_r$ according to (20), where

$$\boldsymbol{\Theta} = \begin{bmatrix} e^{j\theta_1} & 0 \\ 0 & e^{j\theta_2} \end{bmatrix}.$$

However, the desired result in this special case is

$$\boldsymbol{c}(t) = e^{2\pi j t/T} \cdot \boldsymbol{\Phi} \cdot \overline{\mathcal{F}_1(\boldsymbol{i})(t)} \tag{23}$$

where

$$\boldsymbol{\Phi} = \begin{bmatrix} e^{j\phi_1} & 0 & 0 \\ 0 & e^{j\phi_2} & 0 \\ 0 & 0 & e^{j\phi_3} \end{bmatrix}.$$

Equations (17), (20), and (23) are combined to obtain

$$\boldsymbol{c}(t) = \boldsymbol{\Phi}\boldsymbol{H}\boldsymbol{\Theta}' \cdot \boldsymbol{c}_r(t). \tag{24}$$

It follows from (22) and (24) that

$$\boldsymbol{c}(t) = \boldsymbol{\Phi}\boldsymbol{H}(\boldsymbol{M}\boldsymbol{H})^+ \cdot \boldsymbol{b}(t). \tag{25}$$

Therefore the special goal of three-phase delta calibration is to determine the matrix $\boldsymbol{\Phi}\boldsymbol{H}\boldsymbol{\Theta}'$, which is then multiplied by $\boldsymbol{\Theta}(\boldsymbol{M}\boldsymbol{H})^+$ (the result of the previous AC calibration algorithm) to obtain the matrix $\boldsymbol{\Phi}\boldsymbol{H}(\boldsymbol{M}\boldsymbol{H})^+$ which recovers $\boldsymbol{c}(t)$ from $\boldsymbol{b}(t)$.

In a three-phase system, the voltages on any pair of conductors have the same amplitude but are separated in phase by 120 degrees. Thus there are only two possibilities for the phase relationships between the three voltages:

$$\begin{aligned} e^{j\phi_1}/e^{j\phi_3} &= e^{\pm 2\pi j/3} \\ e^{j\phi_2}/e^{j\phi_3} &= e^{\mp 2\pi j/3} \\ e^{j\theta_1}/e^{j\phi_3} &= e^{\pm 5\pi j/6} \\ e^{j\theta_2}/e^{j\phi_3} &= e^{\mp 5\pi j/6}. \end{aligned}$$

and

$$\boldsymbol{\Phi}\boldsymbol{H}\boldsymbol{\Theta}' = \begin{bmatrix} e^{\pm \pi j/6} & 0 \\ 0 & e^{\mp \pi j/6} \\ e^{\mp \pi j/6} & e^{\pm \pi j/6} \end{bmatrix}. \tag{26}$$

All that remains is to determine which signs the exponents take.

Observe that $\boldsymbol{\Phi}\boldsymbol{H}(\boldsymbol{M}\boldsymbol{H})^+$ is the product of a diagonal matrix $\boldsymbol{\Phi}$ and a real-valued matrix $\boldsymbol{H}(\boldsymbol{M}\boldsymbol{H})^+$. Thus every row of $\boldsymbol{\Phi}\boldsymbol{H}(\boldsymbol{M}\boldsymbol{H})^+$ is equal to a complex scalar times a real row vector. However, if the incorrect choice of $\boldsymbol{\Phi}\boldsymbol{H}\boldsymbol{\Theta}'$ is made, the last row of the incorrect $\boldsymbol{\Phi}\boldsymbol{H}(\boldsymbol{M}\boldsymbol{H})^+$ *cannot* be expressed as a complex scalar times a real row vector. This provides a mechanism for deducing the correct value of $\boldsymbol{\Phi}\boldsymbol{H}\boldsymbol{\Theta}'$.

Reference [6] shows that the function

$$r(\boldsymbol{w}) = 1 - \left| \sum_{x=1}^{k} \frac{w_x^2}{\|\boldsymbol{w}\|^2} \right|^2 \tag{27}$$

is equal to 0 if and only if the vector $\boldsymbol{w}$ has elements w_x which are all real multiples of a single complex number, and increases with the angle between the vector's elements in the complex plane. The function r is applied to the two candidates for the bottom row of $\boldsymbol{\Phi}\boldsymbol{H}(\boldsymbol{M}\boldsymbol{H})^+$, and whichever one is closer to zero indicates the correct choice of $\boldsymbol{\Phi}\boldsymbol{H}\boldsymbol{\Theta}'$.

In summary, calibrating a three-phase delta-connected system proceeds as follows:

1) Attach a reference load which draws a constant-amplitude current of β (in phase with the applied voltage) between conductors 1 and 3 and then between conductors 2 and 3.
2) Use (16) to compute $\boldsymbol{b}$ over an interval of time which includes all runs of the reference load.
3) Call the function CALIBRATE$(\boldsymbol{b}, \beta)$. The result is the matrix $\boldsymbol{\Theta}(\boldsymbol{M}\boldsymbol{H})^+$.
4) Use (26) and (27) to determine the correct value of the matrix $\boldsymbol{\Phi}\boldsymbol{H}\boldsymbol{\Theta}'$.
5) Form the product
$$\boldsymbol{\Phi}\boldsymbol{H}(\boldsymbol{M}\boldsymbol{H})^+ = \boldsymbol{\Phi}\boldsymbol{H}\boldsymbol{\Theta}' \cdot \boldsymbol{\Theta}(\boldsymbol{M}\boldsymbol{H})^+.$$
6) To perform regular monitoring of currents, compute $\boldsymbol{b}(t)$ from $\boldsymbol{s}(t)$ using (16). Then multiply by $\boldsymbol{\Phi}\boldsymbol{H}(\boldsymbol{M}\boldsymbol{H})^+$ on the left to obtain $\boldsymbol{c}(t)$.

If (26) and (27) do not clearly indicate which is the correct value of $\boldsymbol{\Phi}\boldsymbol{H}\boldsymbol{\Theta}'$, then the initial assumption of symmetric three-phase power distribution was incorrect.

VI. Eliminating the reference load

In some cases, it is not feasible to attach a special calibration device to each conductor. In a typical energy monitoring appplication, most of the calibration process can be carried out "implicitly" using only the standard electrical devices which are already attached to the conductors. The former requirement that each $\boldsymbol{\sigma}_x$ is equal to β times a column of $\boldsymbol{M}$ is relaxed to allow each $\boldsymbol{\sigma}_x$ to be an arbitrary scalar times a column of $\boldsymbol{M}$. Thus each $\boldsymbol{\sigma}_x$ can be the change in magnetic field due to an arbitrary load switching on, rather than just the change in magnetic field due to a known reference load switching on.

However, the demodulation scheme is no longer applicable for separating the magnetic field due to a particular load from the magnetic fields due to background loads which are operating simultaneously. Instead, $\boldsymbol{s}(t)$ is passed through a high-pass filter and the local extrema of the resulting signal are adopted as the new $\boldsymbol{\sigma}_x$. Since it is very unlikely for independent loads attached to different conductors to switch on or off at exactly the same instant, these values of $\boldsymbol{\sigma}_x$ indeed represent separate columns of $\boldsymbol{M}$. The revised calibration procedure is given in algorithm 2.

Implicit calibration differs from standard calibration in that (i) p may be much larger than n, and (ii) the vectors $\boldsymbol{D}\boldsymbol{\sigma}_x$ in a cluster may have different magnitudes. The

Algorithm 2 Implicit calibration (without a reference load) for direct currents with external path for return current.

Require: the majority of step changes present in $\boldsymbol{s}$ are scaled columns of some matrix $\boldsymbol{M}$, and all columns of $\boldsymbol{M}$ are represented by step changes.

Ensure: $\boldsymbol{K}$ is the pseudoinverse of $\boldsymbol{M}$, up to a permutation of its rows and constant scaling factor applied to each row.

function IMPLICITCALIBRATE($\boldsymbol{s}$, β)
  $\hat{\boldsymbol{s}} \leftarrow$ HIGHPASSFILTER($\boldsymbol{s}$)
  $\boldsymbol{\sigma}_* \leftarrow$ FINDLOCALEXTREMA($\hat{\boldsymbol{s}}$)
  $\boldsymbol{\Sigma} \leftarrow \begin{bmatrix}\boldsymbol{\sigma}_1 & \cdots & \boldsymbol{\sigma}_p\end{bmatrix}$
  $\lambda_*, \boldsymbol{\rho}_* \leftarrow$ EIGENDECOMPOSITION($\boldsymbol{\Sigma}\boldsymbol{\Sigma}'$)
  $n \leftarrow$ COUNTNONZERO($\lambda_1, \ldots, \lambda_k$)
  $\boldsymbol{D} \leftarrow \begin{bmatrix}\boldsymbol{\rho}_1 & \cdots & \boldsymbol{\rho}_n\end{bmatrix}'$
  $\boldsymbol{\delta}_* \leftarrow$ SPECTRALCLUSTER($\boldsymbol{D}\boldsymbol{\sigma}_1, \ldots, \boldsymbol{D}\boldsymbol{\sigma}_p$)
  $\boldsymbol{U} \leftarrow \beta \begin{bmatrix}\boldsymbol{\delta}_1 & \cdots & \boldsymbol{\delta}_n\end{bmatrix}^{-1}$
  $\boldsymbol{K} \leftarrow \boldsymbol{U}\boldsymbol{D}$
  return $\boldsymbol{K}$
end function

former is not important because the eigendecomposition and clustering algorithms scale well to larger datasets. The latter means that $\boldsymbol{U}$ and $\boldsymbol{K}$ can only be determined up to a constant scaling factor multiplying each row. However, in any building that is outfitted with a low-bandwidth utility-provided power meter, the non-contact sensor measurements may be compared with the utility's power measurements over a longer period of time to determine the unknown scaling factors.

VII. RESULTS

In any real application of non-contact sensors, it is impossible to know the matrices $\boldsymbol{M}$ or $\boldsymbol{\Theta}$ in advance. This section begins with a numerical example so that the calibration procedure can be tested with full knowledge of the unknown parameters. Following this analytical demonstration of the algorithm, this section also presents results comparing a non-contact power sensor with a conventional power meter in an actual experiment on a three-phase power service.

Suppose that there are three sensors instrumenting a household service entrance cable with two high-voltage conductors and a neutral return, such that the sensor matrix is given by

$$\boldsymbol{M} = \begin{bmatrix}0.5 & 0.3 & 0.7\\ 0.3 & 0.5 & 0.7\\ 0.4 & 0.4 & 0.8\end{bmatrix}.$$

This poorly-conditioned matrix is typical of service entry cable with a braided neutral conductor surrounding the line conductors, similar to the cable illustrated in Fig. 1.

Further suppose that the line voltages are $2\pi/3$ radians apart, and the reference phase is 0.5 radians behind the first conductor voltage, so that

$$\boldsymbol{\Theta} = \begin{bmatrix}e^{-0.5j} & 0\\ 0 & e^{2\pi j/3 - 0.5j}\end{bmatrix}.$$

The reference load is run four times (twice on each conductor). Each time, it draws an RMS current of $\beta = 2.2\,\mathrm{A}$ between a line conductor and neutral. If the reference load signature $\boldsymbol{\sigma}_x$ corresponds to the yth conductor, then we simulate

$$\boldsymbol{\sigma}_x = \beta e^{-j\theta_y}\boldsymbol{M}(\hat{\boldsymbol{i}}_y - \hat{\boldsymbol{i}}_3) + \boldsymbol{n}_x \tag{28}$$

where $\boldsymbol{n}_x$ is a randomly generated complex noise vector that is scaled to perturb each $\boldsymbol{\sigma}_x$ by about 2%.

Equation (28) is applied to obtain

$$\boldsymbol{\sigma}_1 = \begin{bmatrix}+0.01 + 0.86j\\ -0.01 + 0.43j\\ +0.01 + 0.87j\end{bmatrix} \qquad \boldsymbol{\sigma}_2 = \begin{bmatrix}-0.39 - 0.22j\\ -0.78 - 0.44j\\ -0.76 - 0.43j\end{bmatrix}$$

$$\boldsymbol{\sigma}_3 = \begin{bmatrix}-0.39 - 0.20j\\ -0.78 - 0.43j\\ -0.80 - 0.42j\end{bmatrix} \qquad \boldsymbol{\sigma}_4 = \begin{bmatrix}+0.04 + 0.90j\\ +0.02 + 0.45j\\ +0.02 + 0.87j\end{bmatrix}.$$

The goal of calibration is to determine the matrix $\boldsymbol{\Theta}(\boldsymbol{M}\boldsymbol{H})^+$, which is equal to

$$\begin{bmatrix}+1.81 - 0.99j & -2.58 + 1.41j & -0.52 + 0.28j\\ +0.07 - 2.94j & -0.05 + 2.06j & -0.01 - 0.59j\end{bmatrix}.$$

However, this matrix must be determined using *only* the quantities $\boldsymbol{\sigma}_1$, $\boldsymbol{\sigma}_2$, $\boldsymbol{\sigma}_3$, $\boldsymbol{\sigma}_4$, and β.

First assemble the $\boldsymbol{\sigma}_x$ into $\boldsymbol{\Sigma}$ and compute

$$\boldsymbol{\Sigma}\boldsymbol{\Sigma}' = \begin{bmatrix}1.94 & 1.57 - 0.02j & 2.32 - 0.02j\\ 1.57 + 0.02j & 1.98 & 2.35 + 0.02j\\ 2.32 + 0.02j & 2.35 - 0.02j & 3.09\end{bmatrix}.$$

The eigenvalues of $\boldsymbol{\Sigma}\boldsymbol{\Sigma}'$ are 6.62, 0.40, and 0.001, so $n = 2$. From the eigendecomposition of $\boldsymbol{\Sigma}\boldsymbol{\Sigma}'$, $\boldsymbol{D}$ is given by

$$\begin{bmatrix}-0.51 - 0.00j & -0.52 + 0.01j & -0.68 + 0.01j\\ +0.71 + 0.00j & -0.70 + 0.02j & -0.00 - 0.00j\end{bmatrix}.$$

The clustering algorithm assigns $\boldsymbol{D}\boldsymbol{\sigma}_1$ and $\boldsymbol{D}\boldsymbol{\sigma}_4$ to the first cluster and $\boldsymbol{D}\boldsymbol{\sigma}_2$ and $\boldsymbol{D}\boldsymbol{\sigma}_3$ to the second cluster, with cluster centers

$$\boldsymbol{\delta}_1 = \begin{bmatrix}-0.03 - 1.27j\\ +0.01 + 0.32j\end{bmatrix} \qquad \boldsymbol{\delta}_2 = \begin{bmatrix}+1.14 + 0.61j\\ +0.28 + 0.15j\end{bmatrix}.$$

Therefore

$$\boldsymbol{U} = \beta \begin{bmatrix}\boldsymbol{\delta}_1 & \boldsymbol{\delta}_2\end{bmatrix}^{-1} = \begin{bmatrix}-0.02 + 0.85j & +0.11 - 3.52j\\ +0.76 - 0.41j & +3.06 - 1.62j\end{bmatrix}$$

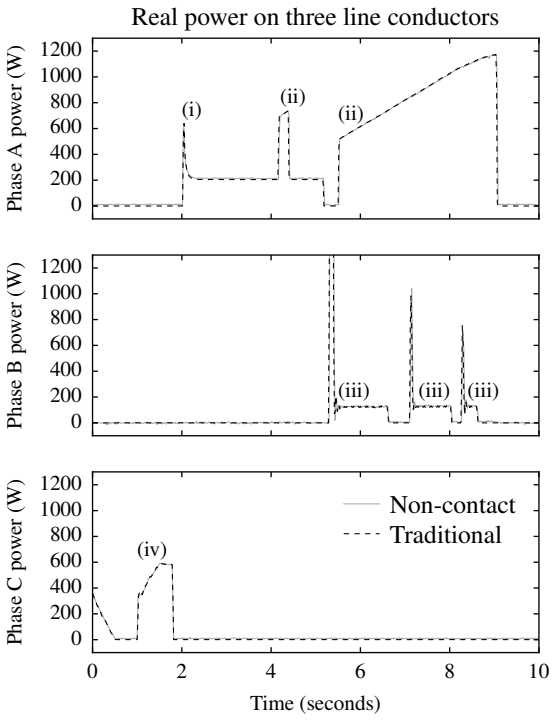

Fig. 4. Data collected by non-contact and traditional power meters. The turn-on transients depicted are from (i) a 250 W incandescent lightbulb, (ii) a 1500 W space heater, (iii) an 0.25 hp induction motor, and (iv) a 600 W bank of dimmable incandescent lightbulbs.

and the matrix $\boldsymbol{UD}$ is equal to

$$\begin{bmatrix} +0.09 - 2.95j & -0.02 + 2.03j & -0.00 - 0.57j \\ +1.80 - 0.95j & -2.51 + 1.40j & -0.54 + 0.28j \end{bmatrix},$$

which differs from the true value of $\boldsymbol{\Theta}(\boldsymbol{MH})^{+}$ by about 2%. This deviation is caused by the noise added to $\boldsymbol{\sigma}_x$. The rows are permuted because the order of clusters is determined arbitrarily, i.e. the two line conductors have no inherent ordering.

Next, the calibration algorithm was tested with the non-contact sensor system shown in Fig. 1 installed on the feeder cable of a three-phase $208/120V$ laboratory electrical service. The service provides power to a collection of electrical loads, including a $250W$ incandescent fixture, a $1500W$ space heater, a quarter horsepower induction motor pump, and a bank of incandescent lamps with a total consumption of $600W$. Along with this "non-contact" system, a "traditional" monitor was installed using high-bandwidth LEM LA-55 current sensors and ohmic LV-25P voltage sensors. This traditional current and voltage monitoring equipment was installed on the AC service entrance cable for comparison.

The non-contact sensors were calibrated using algorithm 1 and the various loads were operated on each of the three line conductors. Voltage phase is determined by the sensors shown in Fig. 1 by the capacitive sensors collocated in each sensor head, permitting the real-time computation of consumed power. The results of this experiment are plotted in Fig. 4. The comparison in Fig. 4 illustrates that the traditional power measurements and the non-contact power measurements agree to better than 1% over a dynamic range of $1000\,\mathrm{W}$.

VIII. Conclusion

The algorithms introduced in this paper permit easy installation and calibration of non-contact power meters. Since the calibration algorithm can handle overconstraint in both the number of sensors and also the number of calibration measurements, it is not necessary to know *a priori* the precise number of conductors in a wire bundle, as long as an upper bound is known. Knowledge of the wire and sensor geometry is not required in order to obtain accurate calibration and measurement results.

Our preliminary field experiments have uncovered residential and commercial sites where conventional assumptions about the power wiring do not hold. For example, we have found homes where signifcant currents flow or return down the earth or safety ground in a home. Work is underway to extend the analysis illustrated in Fig. 3 to provide automatic detection and reporting of these "stray" or unexpected currents outside of the conventional service connections.

References

[1] J. S. Donnal and S. B. Leeb, "Noncontact power meter," *IEEE Sensors J.*, vol. 15, pp. 1161–1169, Feb. 2015.

[2] J. Lenz and A. S. Edelstein, "Magnetic sensors and their applications," *IEEE Sensors J.*, vol. 6, pp. 631–649, Jun. 2006.

[3] P. Pai, C. Lingyao *et al.*, "Non-intrusive electric power sensors for smart grid," in *Proc. IEEE Sensors*, Oct. 2012, pp. 1–4.

[4] E. J. M. van Heesch, R. Caspers *et al.*, "Three phase voltage measurements with simple open air sensors," in *Proceedings of the 7th International Symposium on High Voltage Engineering*, Aug. 1991.

[5] K. T. Selva, O. A. Forsberg *et al.*, "Non-contact current measurement in power transmission lines," *Procedia Technology*, vol. 21, pp. 498–506, Aug. 2015.

[6] D. Lawrence, "Hardware and software architecture for non-contact, non-intrusive load monitoring," Master's thesis, Massachusetts Institute of Technology, Feb. 2016.

[7] U. von Luxburg, "A tutorial on spectral clustering," *Statistics and Computing*, vol. 17, pp. 395–416, Dec. 2007.